Available online at www.sciencedirect.com
SCIENCE DIRECT®
Journal of Catalysis 221 (2004) 601–611
JOURNAL OF CATALYSIS
www.elsevier.com/locate/jcat

Characteristics of chromium oxides supported on TiO_2 and Al_2O_3 for the decomposition of perchloroethylene

Sung Dae Yim and In-Sik Nam *

Department of Chemical Engineering/School of Environmental Science and Engineering, Pohang University of Science and Technology (POSTECH), San 31 Hyoja-Dong, Pohang 790-784, Republic of Korea

Received 12 May 2003; revised 18 September 2003; accepted 29 September 2003

Abstract

The effects of supports including TiO_2 and Al_2O_3 on the molecular structure and catalytic activity of chromium oxide for the complete oxidation of perchloroethylene (PCE) have been examined with respect to the content of Cr on the catalyst surface. The results from XRD, XPS, Raman, and TPR-TPO indicate that the state of the surface species of chromium oxide strongly depends on catalyst support and Cr loading. The amount of Cr(VI) in the high oxidation state on the surface of the catalyst increased as the content of Cr increased from 1 to 17 wt%, while the relative ratio of Cr(VI)/Cr(III) existing on the catalyst surface decreased with respect to the Cr loading, regardless of the supports examined in the present study. The molecular structure of Cr(VI) was also altered with respect to the content of Cr and the surface nature of support. Monochromate species appeared on the surface of Al_2O_3 at 1 wt% of Cr loading on the catalyst surface. However, further increase in the Cr contents up to 17 wt% formed di-, tri-, and tetrachromate species of Cr(VI) and crystalline α-Cr_2O_3 on the surface of Al_2O_3. CrO_x/TiO_2 catalyst formed polymeric chromium oxide species on its surface in the wide range of Cr content of the catalyst from 1 to 17.4 wt%. The high degree of polymerization of chromate species on the surface of TiO_2 containing the strong redox ability is contrasted with the state of the chromate species on Al_2O_3. The rate of PCE oxidation was enhanced as the Cr loading increased for both catalysts. CrO_x/TiO_2 catalyst revealed a relatively higher reaction rate than CrO_x/Al_2O_3 at the given content of Cr and its surface density. TOF of the catalyst increased along with the degree of polymerization of the chromate species on the catalyst surface. The superior performance of CrO_x/TiO_2 catalyst is attributed mainly to the formation of the polychromate species containing a stronger redox ability on the surface of TiO_2. This clearly suggests that the metal–oxygen–support interaction (MOSI) is critical in the present catalytic reaction system.

Keywords: Chromia; Titania; Alumina; Chlorinated hydrocarbons; Oxidation

1. Introduction

Chromium-based catalysts have been widely examined for polymerization, hydrogenation-dehydrogenation, isomerization, aromatization, partial oxidation, and $DeNO_x$ reaction because of the peculiar characteristics of Cr oxide species on the surface of the support, including oxidation state, coordination environment, and degree of polymerization [1]. This versatility of the supported chromium oxide catalyst has led to extensive fundamental studies on the parameters controlling the molecular structure of chromium oxide on the catalyst surface. The catalyst characterization techniques employed were mainly Raman [2–15], IR [15,16], XPS [17–24], ESR [25], TPR [26–31], and EXAFS-XANES [32–35]. Deo and Wachs [13] investigated the combined molecular structure of chromium oxide containing both mono- and polychromate to elucidate the performance of 1 wt% chromium-based catalysts for methanol oxidation. The catalytic activity was closely related to the surface oxide–support interaction, and the role of the support was also critical for the reaction system revealing the reactivity in the order of $CrO_x/ZrO_2 > CrO_x/TiO_2 > CrO_x/SiO_2 > CrO_x/MgO > CrO_x/Nb_2O_5 > CrO_x/Al_2O_3$. Recently, Fountzoula et al. [20] reported that the creation of the monochromate species on the surface of the anatase-type TiO_2 is important for high performance of the $deNO_x$ reaction. However, there have been few studies clearly elucidating the roles of the surface chromate species and the supports in the oxidation reactions, particularly the removal of chlorinated hydrocarbon, perchloroethylene (PCE) in the present study. PCE has been commonly employed as a stan-

* Corresponding author.
E-mail address: isnam@postech.ac.kr (I.-S. Nam).

0021-9517/$ – see front matter
doi:10.1016/j.jcat.2003.09.026

dard compound for the development of the catalytic system for the removal of CVOCs (chlorinated volatile organic compounds) [36].

There have been a number of investigations on the catalytic oxidation of CVOCs, regarded as one of the major air pollutants. The catalytic process contains a variety of distinctive advantages, including mild operating conditions, low energy consumption, and less formation of noxious byproducts over incineration and sorption as a CVOC removal technology. The catalyst developed so far is mainly noble metal or metal oxide [37]. It has been reported that among the catalysts chromium oxide is the most effective for the complete oxidation of PCE [38]. Moreover, CrO_x/TiO_2 and $/Al_2O_3$ catalysts containing a high surface area revealed the strongest PCE removal activity compared to the chromium oxides supported on SiO_2, SiO_2–Al_2O_3, activated carbon, and low surface area of TiO_2 and Al_2O_3 [39]. It was also concluded that the high performance of CrO_x/TiO_2 and $/Al_2O_3$ is primarily due to the formation of a high amount of Cr(VI), the active reaction species on the surface of the support. However, the distinction of the PCE removal activity over CrO_x/TiO_2 and $/Al_2O_3$ catalysts could not be well understood simply with the amount of Cr(VI) formed on the catalyst surface at the given density of the hydroxyl group on the surface of the support, which is closely related to the formation of Cr(VI) [3]. It can be anticipated that the molecular structure of Cr(VI) on TiO_2 and Al_2O_3 is also critical for PCE oxidation as well as the amount of Cr(VI) on the catalyst surface. Hence, a systematic study on the molecular structure of chromium oxide with respect to the surface nature of supports and Cr content may be desirable to clearly describe the phenomena occurring on the surface of chromium oxides during the course of the reaction. Although many studies have been reported on the surface structure of CrO_x/TiO_2 and $/Al_2O_3$ catalysts, none of them could observe the distinction of the phase of CrO_x on the surface of TiO_2 and $/Al_2O_3$ containing a variety of the metal contents and they simply discussed that both supports form a similar molecular structure of chromium oxide compared to that on the surface of SiO_2. Moreover, the correlation of the catalytic oxidation, particularly decomposition of CVOC with the molecular structure and the redox property of CrO_x has not been examined yet.

In the present study, the role of TiO_2 and Al_2O_3 supports for the characteristics of chromium oxide including the molecular structure, the redox ability, and the catalytic activity for the complete oxidation of PCE was investigated and compared in order to elucidate the correlation between the characteristics of the catalyst and its activity. XRD, XPS, Raman, and TPR-TPO were employed to investigate the surface structure of chromium oxide species and redox property of the catalysts, and TOF was also calculated on the basis of the steady-state oxidation rate of PCE examined in a continuous flow reactor system. Then, the high performance of CrO_x/TiO_2 catalyst over CrO_x/Al_2O_3 for the removal of CVOC has been thoroughly understood.

2. Experimental

The supported chromium oxide catalysts were prepared by the incipient wetness impregnation method with an aqueous solution of chromium nitrate [$Cr(NO_3)_3 \cdot 9H_2O$, Aldrich Chemical Co.]. The supports employed in the present study were TiO_2 (Hombikat UV-100) and Al_2O_3 (Aldrich) containing the highest PCE removal activity confirmed in an earlier study [39]. Both supports also contain similar surface areas, 250 and 290 m^2/g, respectively. After the impregnation of chromium oxide on the supports, the catalysts were subsequently dried at 110 °C for 12 h and calcined in air at 450 °C for 5 h. The BET surface areas of the catalysts were measured with a Micromeritics ASAP 2010 using liquid N_2 at 77 K. Prior to the measurements, the catalysts were pretreated in vacuo at 180 °C for 10 h.

XRD patterns of the catalyst prepared in the present study were observed by an M18XHF (MAC Science Co.) diffractometer employing Cu-K_α radiation ($\lambda = 1.5405$ Å) as an X-ray gun. The diffraction patterns in the regions of $2\theta = 10$–$90°$ were usually examined with a scanning speed of 4.0°/min, operating at 40 kV and 200 mA of an X-ray gun.

XPS spectra were obtained by VG ESCALAB 220i equipped with Mg anode (Mg-K_α radiation, 1253.6 eV) run at 15 kV and 20 mA. The spherical sector of the analyzer was operated in the fixed transmission (FAT) mode with a pass energy of 50 eV set across the hemispheres. The instrument was typically operated at a pressure near 1×10^{-8} Torr in the analysis chamber. The samples of the catalyst were analyzed in a powder dusted on a double-sided adhesive tape. The oxidation state of chromium existing on the catalyst surface was determined by curve fitting using nonlinear least squares with the Cr $2p_{3/2}$ envelope. The binding energies of XPS results for the catalyst samples were referenced with the C 1s line (284.6 eV) of the carbon overlayer. The full widths of the peak at the half-maximum (FWHM) were allowed to change to attain the best fitting. The positive charge produced during the photoejection process was compensated by a flood gun. In order to minimize the photoreduction of chromium oxide species on the catalyst surface during XPS experiments, all the catalyst samples were analyzed within a short period of time. To calculate the theoretical ratio of the peak intensities for Cr 2p/Ti 2p and Cr 2p/Al 2p, the model developed by Kerkhof and Moulijn [40] was employed. The model has been widely employed to demonstrate the maximum concentration of promoter homogeneously supported on porous material and to predict XPS relative intensity between promoters and supports. Indeed, the model effectively described the ratios of both CrO_x/TiO_2 and CrO_x/Al_2O_3 catalytic systems [16,41]. The cross sections and the mean escape depths of the photoelectrons used for the calculation of the ratio were based upon the previous studies by Scofield [42] and Penn [43], respectively.

Temperature-programmed reduction (TPR) experiments were carried out using 50 mg of the catalysts heated at

10 °C/min under hydrogen (5%) atmosphere in a flow of nitrogen at 40 ml/min. The catalysts were pretreated with oxygen at 500 °C for 0.5 h. A thermal conductivity detector (TCD; HP 5890 GC) was employed to examine the consumption of hydrogen during the reduction of the catalyst. The reducing gas mixtures were dried in a cold trap before reaching TCD of GC. Temperature-programmed oxidation (TPO) spectra were also obtained with the identical apparatus employed for the TPR study over the reduced catalysts using oxygen (1%) in a flow of helium. The TPO experiment was performed with the reduced catalyst during TPR, and TPR was conducted again after TPO. Hence, the TPR-TPO-TPR experiment was done in series to understand the reduction and reoxidation property of the chromium oxide catalysts.

Raman spectra were recorded from the powder sample pressed into self-supporting wafers. The spectra were obtained in the 180° configuration on a Model 532-RENS-A01, using the 514.5-nm radiation of argon ion gas as an excitation source. The laser power at the sample wafers was 25 mW, and the spectral resolution was 3–4 cm^{-1}. The scattered radiation was detected by a Wright instrument containing an intensified photodiode array, cooled thermoelectrically to −30 °C. The Raman spectra were obtained at room temperature and under ambient conditions.

The conversion and the reaction rate of the complete oxidation of PCE were examined in a continuous flow microreactor by using 0.03–0.3 g of 60/80 mesh size of the catalysts diluted in inert quartz in order to avoid the reactant channeling under atmospheric pressure. A reactant mainly containing air with 30 ppm of PCE was fed into the reactor at a flow rate of 600 ml/min. The feed and product streams of the reactor were analyzed by on-line Hewlett-Packard 5890A gas chromatography (GC) with TCD and FID detectors. The steady-state conversion of PCE was calculated by measurement of the inlet and outlet concentrations of PCE at 300 °C. No chlorinated by-products were detected in the downstream of the reactor during the course of reaction. HCl and Cl_2 were not detected due to the detection problems in the product stream. It has been confirmed by carbon balance, however, that more than 90% of PCE mainly converted to CO and CO_2. The detailed experimental procedures were already described elsewhere [39].

3. Results

The surface area and density of chromium oxide catalysts employed in the present study are listed in Table 1 as a function of Cr content on TiO_2 and Al_2O_3. The density is defined as the number of chromium atoms per square nanometer of the surface area of the catalyst. The catalysts are represented by x symbols of CrO_x/Al_2O_3 or $/TiO_2$, where x is the Cr content on the catalyst. The impregnation of chromium on the surface of the supports decreased the specific surface area of the support as the content of Cr increased due to the blocking of relatively narrow pores of the supports by chromium oxide [20]. The higher the content of Cr on the surface of the support, the higher the surface densities of chromium atoms attained. Monolayer surface coverage of supported chromium is known as 6.6 and 4.0 atoms/nm^2 of the surface density for TiO_2 and Al_2O_3, respectively, by Raman spectroscopy discriminating the phase of CrO_x in the forms of two-dimensional overlayer and crystallites [15]; hence the catalysts contain approximately 0 to 2.7 of theoretical monolayer of Cr on the surface of the support.

Table 1
Chromium content, surface area, and chromium oxide surface density for CrO_x/TiO_2 and $/Al_2O_3$ catalysts

Catalyst	Cr content (wt%)	BET surface area (m^2/g)	CrO_x surface density (nm^{-2})
TiO_2	–	250	–
$1CrO_x/TiO_2$	1.0	217	0.5
$3.2CrO_x/TiO_2$	3.2	228	1.6
$5.1CrO_x/TiO_2$	5.1	212	2.8
$11.9CrO_x/TiO_2$	11.9	177	7.8
$17.4CrO_x/TiO_2$	17.4	153	13.2
Al_2O_3	–	290	–
$1CrO_x/Al_2O_3$	1.0	262	0.4
$3.3CrO_x/Al_2O_3$	3.3	268	1.4
$5CrO_x/Al_2O_3$	5.0	251	2.4
$10.8CrO_x/Al_2O_3$	10.8	232	5.4
$16.8CrO_x/Al_2O_3$	16.8	184	10.6

3.1. XRD

Fig. 1 shows the XRD patterns of supported chromium oxide catalysts with respect to the Cr contents. Most of the diffraction patterns are the characteristic peaks for γ-Al_2O_3 or anatase–TiO_2 without the presence of those of crystalline α-Cr_2O_3 on their surface. The XRD patterns revealing α-Cr_2O_3 appear only for $17.4CrO_x/TiO_2$ catalyst containing the highest Cr content. The results imply that the chromium oxide is well dispersed on the support surface as an amorphous or microcrystalline phase without altering the phase of support, and that crystalline α-Cr_2O_3 only forms on the surface of TiO_2 containing a high content of Cr, $17.4CrO_x/TiO_2$.

3.2. XPS

The XPS patterns of the Cr 2p doublet for both CrO_x/TiO_2 and $/Al_2O_3$ catalysts with respect to the Cr loading can be observed in Fig. 2. The deconvolution of the Cr $2p_{3/2}$ signals based upon the previous studies [17–24] and the comparison to the reference samples including CrO_3 and Cr_2O_3 indicate that the spectra for the present catalytic systems contain two major peaks at 579.3–579.5 eV for Cr(VI) and 576.3–576.9 eV for Cr(III). Although the presence of the intermediate chromium species including Cr(IV) and/or Cr(V) cannot be excluded, the species is hardly distinctive due to the intrinsic complexity of the Cr(III) species by XPS [20].

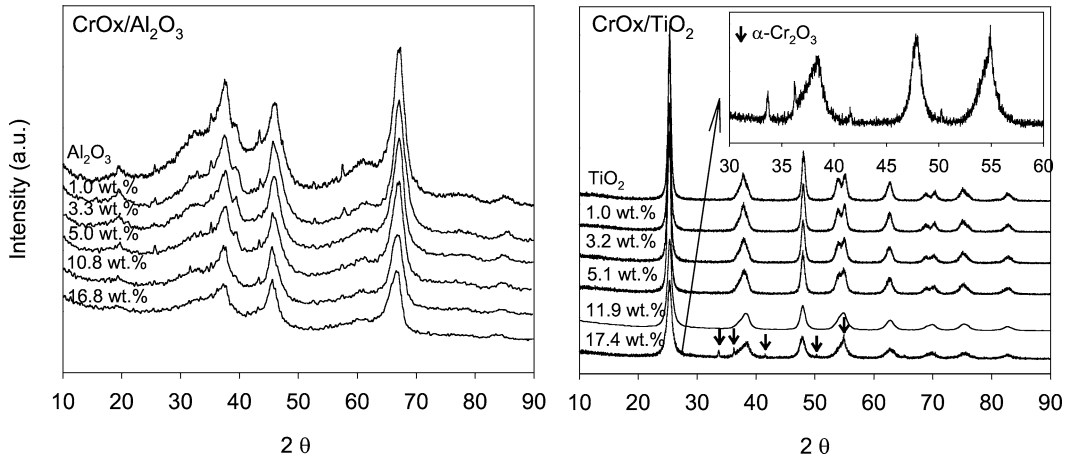

Fig. 1. XRD patterns of CrO_x/TiO_2 and $/Al_2O_3$ catalysts.

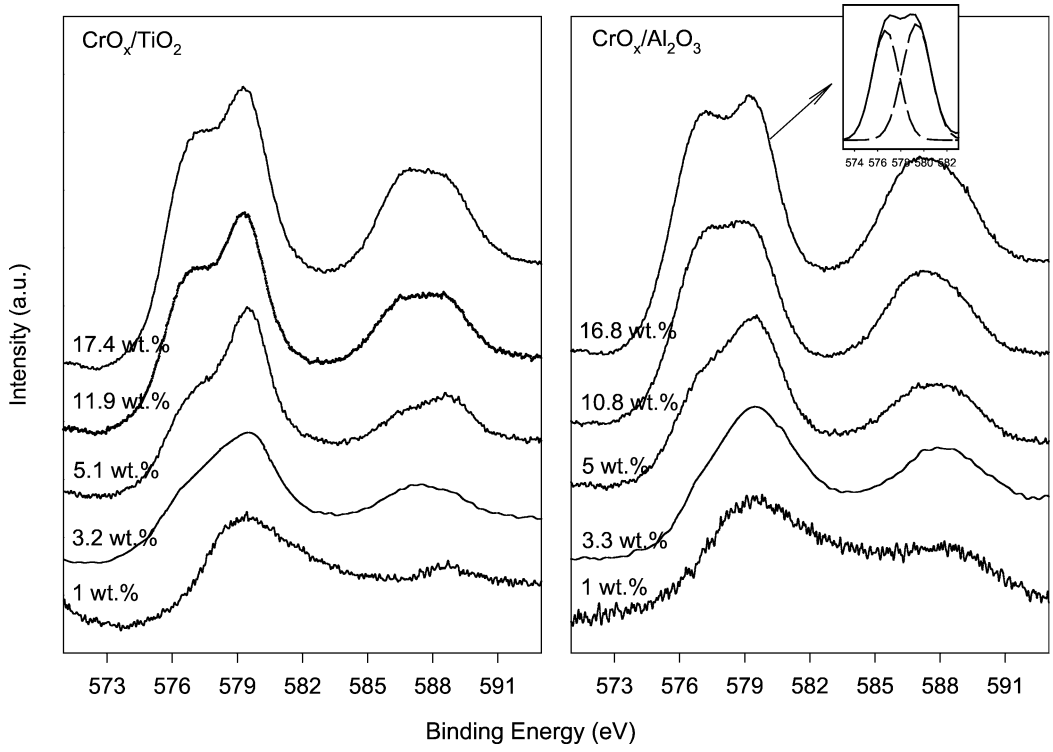

Fig. 2. XPS spectra of CrO_x/TiO_2 and $/Al_2O_3$ catalysts.

XPS spectra of two types of chromium oxide catalysts supported on TiO_2 and Al_2O_3 reveal similar patterns of the response signal without a major distinction with respect to the support. The spectra exhibit that the intensity of the shoulder peak at lower binding energy, which can be assigned to that of Cr(III), increases as the content of Cr on both CrO_x/TiO_2 and $/Al_2O_3$ catalysts increases. The ratios of Cr(VI)/Cr(III) for CrO_x/Al_2O_3 catalyst representing the relative amounts of Cr(VI) and Cr(III) on the catalyst surface based on the peak intensities of XPS for Cr(VI) and Cr(III) decrease with respect to the content of Cr up to 16.8 wt% as listed in Table 2. Although it is expected that the trend of the ratio over CrO_x/TiO_2 with regard to the Cr content is similar to that for CrO_x/Al_2O_3, the intensity ratios for CrO_x/TiO_2 cannot be obtained due to the overlap between a Ti 2s shakeup satellite and the Cr 2p lines [16].

The intensity ratios of Cr 2p/Al 2p and Cr $2p_{3/2}$/Ti $2p_{3/2}$ estimated from XPS observation as a function of the atomic ratios, Cr/Al and Cr/Ti of the catalysts, can be observed in Fig. 3. For CrO_x/TiO_2 catalyst, the ratios of the peak areas for Cr $2p_{3/2}$/Ti $2p_{3/2}$ can be hardly measured due to the overlap between a Ti 2s shakeup satellite (Ti $2s_{sat}$) as stated, which exists at about 13 eV on the high energy side of the Ti 2s, and the Cr 2p line [16]. However, the Cr $2p_{3/2}$/Ti $2p_{3/2}$ area ratio can be obtained by measuring the peak intensity for Cr 2p + Ti $2s_{sat}$ and subtracting the

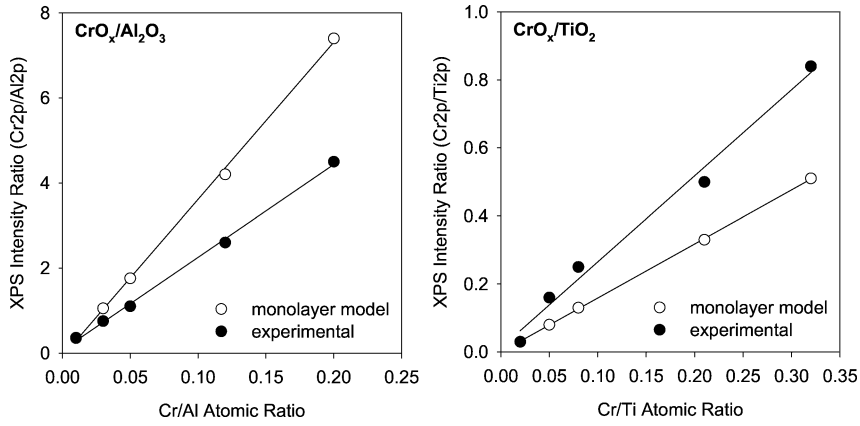

Fig. 3. XPS intensity ratios of Cr 2p/Al 2p and Cr $2p_{3/2}$/Ti $2p_{3/2}$ for CrO_x/TiO_2 and $/Al_2O_3$ catalysts.

intensity for Ti $2s_{sat}$ as estimated from the identical spectra, which was examined on pure TiO_2 by using the intensity of the Ti $2p_{3/2}$ with a weight factor of 0.15 [16]. For comparison, the theoretical value of the Cr 2p/Al 2p and Cr $2p_{3/2}$/Ti$2p_{3/2}$ intensity ratio calculated for monolayer dispersion can also found in Fig. 3.

The intensity ratios between the Cr 2p peak and the Al 2p and Ti 2p peaks increase linearly with respect to the Cr content, indicating that the chromium oxide is well dispersed on the surface of TiO_2 and Al_2O_3 up to 16.8 wt%, although the species of chromium oxides formed on the catalyst surface are transformed from Cr(VI) to Cr(III) as previously confirmed in Table 2. The intensity ratios of Cr 2p/Al 2p and Cr $2p_{3/2}$/Ti $2p_{3/2}$ measured for CrO_x/Al_2O_3 and $/TiO_2$ are identical to that of the theoretical value calculated for monolayer dispersion up to 1 wt% of the Cr content. Above this loading of Cr, the deviation between the measured and the theoretical values begins to occur. For CrO_x/Al_2O_3 catalysts, the Cr 2p/Al 2p intensity ratios are lower than those of monolayer dispersion, and the deviation becomes larger as the Cr loading increases, mainly due to the decrease of chromium oxide dispersion on the catalyst surface. Indeed, the dispersion of CrO_x/Al_2O_3 catalyst was calculated from the result by the XPS, and is listed in Table 2. On the other hand, the Cr $2p_{3/2}$/Ti $2p_{3/2}$ intensity ratios for CrO_x/TiO_2 catalysts are higher than the monolayer values, contrary to the CrO_x/Al_2O_3. This indicates that the present CrO_x/TiO_2 catalytic system may not be described by the Kerkhof–Moulijn monolayer model [16].

Table 2
XPS data for CrO_x/TiO_2 and $/Al_2O_3$ catalysts

Catalyst	Binding energy Cr $2p_{3/2}$ (eV)		Intensity ratio		Dispersion (%)
	Cr(VI)	Cr(III)	Cr 2p/ (Ti, Al) 2p	Cr(VI)/ Cr(III)	
$1CrO_x/TiO_2$	597.4	576.4	0.03	–	–
$3.2CrO_x/TiO_2$	579.4	576.9	0.16	–	–
$5.1CrO_x/TiO_2$	579.5	576.9	0.25	–	–
$11.9CrO_x/TiO_2$	579.3	576.7	0.50	–	–
$17.4CrO_x/TiO_2$	579.3	576.7	0.84	–	–
$1CrO_x/Al_2O_3$	579.3	576.3	0.36	7.7	100
$3.3CrO_x/Al_2O_3$	579.4	576.7	0.75	4.5	71.4
$5CrO_x/Al_2O_3$	579.5	576.9	1.10	2.2	62.5
$10.8CrO_x/Al_2O_3$	579.3	576.9	2.60	1.4	61.9
$16.8CrO_x/Al_2O_3$	579.4	576.8	4.50	1.2	60.8

3.3. Raman

The Raman spectra of CrO_x/Al_2O_3 catalysts containing 1–16.8 wt% of Cr are shown in Fig. 4. For the catalyst containing 1 wt% of Cr, Raman peaks are mainly observed at a band frequency ∼860 and 364 cm^{-1}. These peaks have been assigned to the symmetric stretching and bending modes of isolated tetrahedral surface-chromate species that is distorted by its interaction with the surface of the oxide support [3]. When the Cr content increased to 3.3 wt%, the stretching and bending modes shifted upward to 870 and 374 cm^{-1}, respectively. Although the band at ∼217 cm^{-1} attributed to the presence of Cr–O–Cr linkages is not observed in the present study, the upward shift of the Raman bands indicates the formation of the dimers of chromium oxide [3]. The Raman spectra for $5CrO_x/Al_2O_3$ also show that the bands at ∼874 and ∼378 cm^{-1} corresponding to a dimeric chromium oxide species shift to the higher frequency and contain new peaks at ∼990 and ∼855 cm^{-1}.

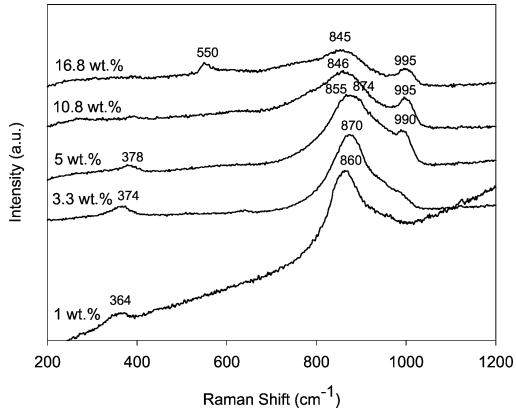

Fig. 4. Raman spectra of CrO_x/Al_2O_3 catalyst.

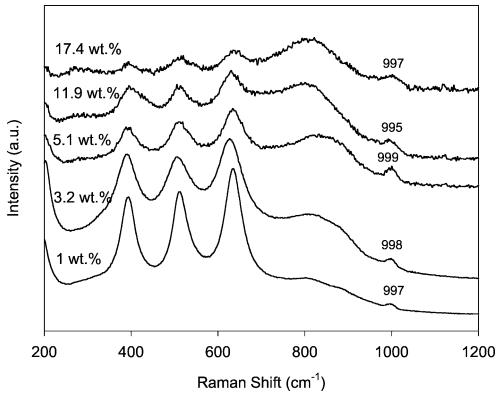

Fig. 5. Raman spectra of CrO_x/TiO_2 catalyst.

This pair of peaks can be commonly assigned to the tri- and tetramers of the chromium oxide by observing the presence of nonterminal chromate units on the catalyst surface [2–5].

The Raman spectra for $5CrO_x/Al_2O_3$ reveal that the chromium oxide exists in the forms of di-, tri-, and tetrameric species on the surface of Al_2O_3. For $10.8CrO_x/Al_2O_3$ catalyst, the spectra exhibit mainly two bands at $\sim$995 and $\sim$846 cm^{-1}, which can be assigned to the polymeric surface species of Cr as discussed. For $16.8CrO_x/Al_2O_3$, a new band appears at $\sim$550 cm^{-1} in addition to the bands at $\sim$995 and $\sim$845 cm^{-1}. The band at this frequency can be commonly assigned to crystalline α-Cr_2O_3 [6]. It should be noted that the decrease of the peak intensity is primarily due to the gradual color change of the catalyst from bright yellow to dark brown as the content of Cr increases on the catalyst surface.

Fig. 5 exhibits the Raman spectra of 1–17.4 wt% CrO_x/TiO_2 catalysts. The strong TiO_2 Raman bands below the frequency at 700 cm^{-1} prevent the examination of the state of chromium oxide in this region of the spectra [3]. Moreover, the second Raman band for the anatase type of TiO_2 at about 800 cm^{-1} also hinders the chromium oxide peaks from the spectra [7]. However, all Raman bands for CrO_x/TiO_2 catalyst examined in the present study reveal that the peak at $\sim$997 cm^{-1} originated from tri- and tetrameric chromium oxide species, which are also observed in the Raman bands for CrO_x/Al_2O_3 catalysts containing high loadings of Cr above 5 wt%.

3.4. TPR-TPO

TPR profiles for chromium oxide catalysts supported on Al_2O_3 and TiO_2 were obtained from 100 to 500 °C to investigate the reducibility of the catalysts as shown in Fig. 6. The reduction feature of the catalyst by hydrogen varies with respect to the type of support and the Cr content of the catalyst. For the CrO_x/Al_2O_3 catalyst, a single reduction peak at 320–390 °C with respect to the Cr content can be observed, whereas the CrO_x/TiO_2 catalyst contains two distinctive reduction peaks at 280–320 (low-temperature peak, LTP) and at 420–440 °C (high-temperature peak, HTP). The maximum of the hydrogen consumption peak for CrO_x/Al_2O_3 shifts toward lower temperatures as the Cr content increases up to 10.8 wt% and then remains at the same temperature even by a further increase of the content to 16.8 wt%. For the CrO_x/TiO_2 catalyst, the intensity of LTP significantly increases compared to HTP as the content of Cr on the catalyst surface increases. In addition, a shift of LTP has been observed to a lower temperature with respect to the content of Cr, although the maximum peak position hardly moves, probably due to the broadening of LTP. The total amount of H_2 consumption by TPR increases as the Cr content increases, regardless of the catalyst support. However, the amount of hydrogen based upon the Cr loading of the catalysts decreases as listed in Table 3.

TPO has been sequentially conducted for the fully reduced chromium oxide catalysts by TPR study within a temperature range from 100 to 550 °C, to verify the reoxidation feature of chromium oxide catalysts. However, TPO profiles within the temperature range covered in the present study were hardly distinctive for examining the reoxidation ability of CrO_x/Al_2O_3 and $/TiO_2$ catalysts, mainly due to the broadness of the patterns. The profiles simply reveal the increase of the amount of oxygen consumption as the Cr content increases. This, however, is quite consistent with the trend of TPR of the catalyst examined.

The reoxidized chromium oxide catalyst by TPO was reduced again by TPR to confirm the reversibility of its redox capability. The spectra by the second TPR (TPR2) for CrO_x/Al_2O_3 and $/TiO_2$ catalysts were similar to those by the first TPR (TPR1), regardless of the contents of Cr on the catalyst surface covered in the present study, while the amount of hydrogen consumption during TPR2 was in the range of 70–80% of that by TPR1.

The redox ability of CrO_x/Al_2O_3 and $/TiO_2$ catalysts was also investigated by hydrogen pulse experiment. The pulse of 8.12 μmol H_2 was fed into the microreactor containing 150 mg of the chromium oxide catalysts with respect to the reduction temperature and the consumption of hydrogen was monitored by TCD. The fixed fraction of hydrogen injected was consistently consumed during the course of the pulse experiment until the surface of the catalyst was fully saturated with H_2 and reduced to Cr(III). The rate of hydrogen con-

Table 3
TPR data for CrO_x/TiO_2 and $/Al_2O_3$ catalysts

Catalyst	T_{max} (°C)		H_2 consumption (a.u.)	H_2/Cr (a.u.)
$1CrO_x/TiO_2$	300	440	282	5.42
$3.2CrO_x/TiO_2$	280	420	440	2.64
$5.1CrO_x/TiO_2$	288	420	520	1.96
$11.9CrO_x/TiO_2$	316	430	750	1.21
$17.4CrO_x/TiO_2$	316	430	753	0.83
$1CrO_x/Al_2O_3$	390	–	187	3.60
$3.3CrO_x/Al_2O_3$	346	–	386	2.25
$5CrO_x/Al_2O_3$	333	–	618	2.38
$10.8CrO_x/Al_2O_3$	325	–	823	1.47
$16.8CrO_x/Al_2O_3$	324	–	903	1.03

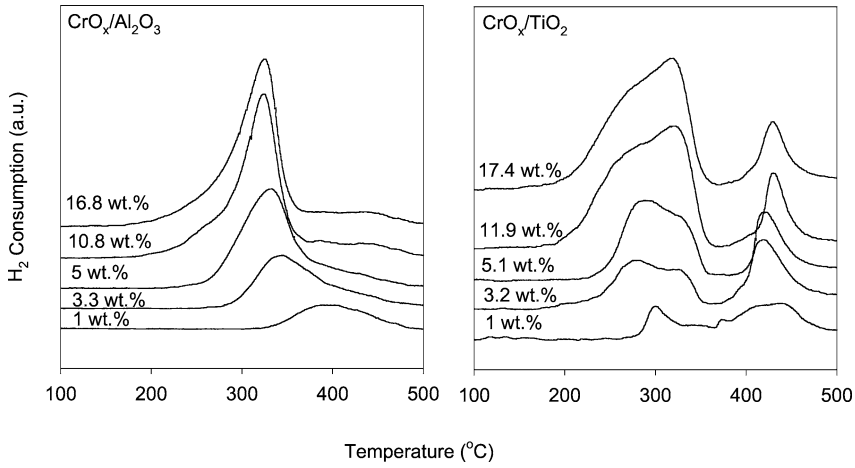

Fig. 6. TPR profiles of CrO_x/TiO_2 and $/Al_2O_3$ catalysts.

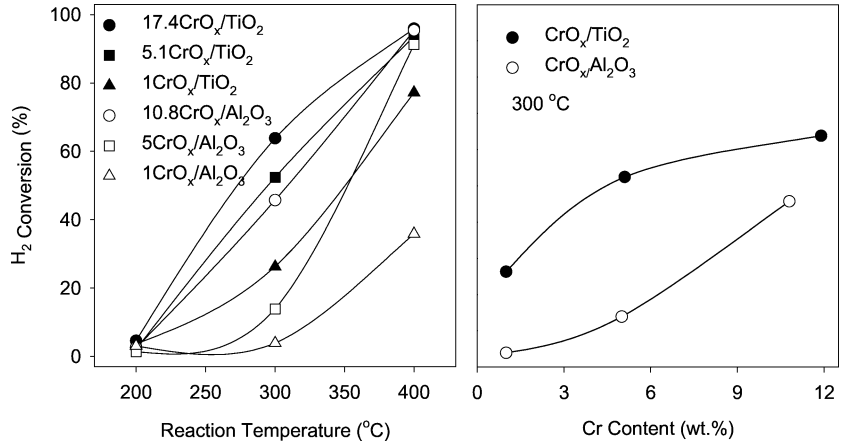

Fig. 7. H_2 conversion of CrO_x/TiO_2 and $/Al_2O_3$ catalysts.

sumption, also regarded as the catalyst reduction rate, can be observed in Fig. 7 with respect to reaction temperature and Cr content. Less than 5% of H_2 injected was consumed at 200 °C, regardless of the catalyst. However, the amount of the consumption increases as the temperature increases and most of hydrogen injected to the catalyst has been consumed at 400 °C except 1 wt% CrO_x/Al_2O_3 and $/TiO_2$. A larger amount of H_2 consumption for CrO_x/TiO_2 has been observed compared to that for CrO_x/Al_2O_3, regardless of the Cr content and reduction temperature. It should be noted that the consumption of H_2 increases as the Cr content increases.

On the other hand, the O_2 pulse experiment revealed distinctive reoxidation phenomena compared with the H_2 pulse test. All of oxygen injected by pulse was completely consumed independent of the oxidation condition until the reduced catalyst was saturated with O_2 and fully reoxidized. Therefore, the reoxidation ability of CrO_x/TiO_2 and $/Al_2O_3$ catalysts can be hardly distinctive by the O_2 pulse experiment.

As another method for the evaluation of the reoxidation rate of the catalyst, the fully reduced chromium oxide catalysts under H_2 at 450 °C for 2 h were reoxidized in air at 200, 300, and 400 °C of the reoxidation temperatures during 2 h of the period, and then the reoxidized catalysts were reduced again by TPR as shown in Fig. 8. The TPR profiles of $11.9CrO_x/TiO_2$ show that the intensity of the two peaks simultaneously increases as the reoxidation temperature increases without alteration of the peak position. The TPR profiles of $10.8CrO_x/Al_2O_3$ also exhibit that the amount of the hydrogen consumption increases with increasing reoxidation temperature, although the maximum reduction temperature, slightly shifts to a higher temperature than before. However, the reoxidation ability of both catalysts is quite distinctive. The $11.9CrO_x/TiO_2$ catalyst reoxidized at 200, 300, and 400 °C restored 22, 61, and 90% of its initial fraction of hydrogen consumption, respectively, during TPR, while the $10.8CrO_x/Al_2O_3$ catalyst did 23, 38, and 50% of its initial hydrogen consumption, respectively. This may indicate that the reoxidation ability of CrO_x/TiO_2 catalyst is stronger than that of CrO_x/Al_2O_3.

3.5. PCE decomposition activity

The conversion of PCE for prereduced $11.9CrO_x/TiO_2$ and $10.8CrO_x/Al_2O_3$ catalysts under H_2 at 450 °C for 2 h

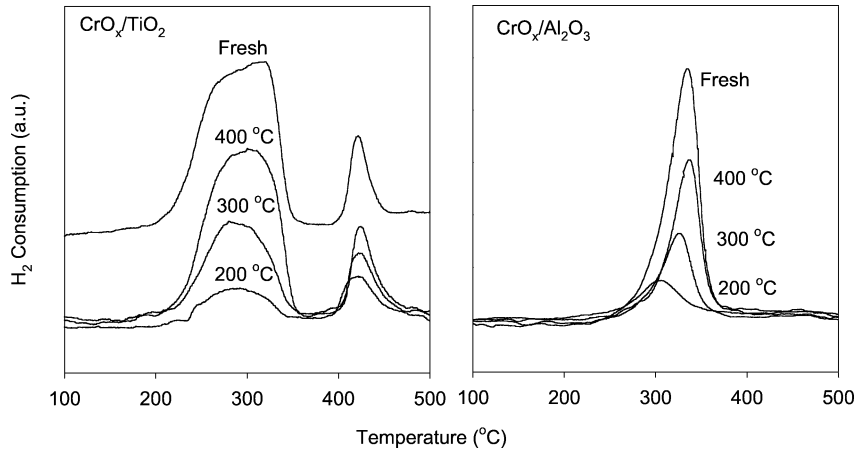

Fig. 8. TPR profiles of fresh and reoxidized 11.9CrO_x/TiO_2 and 10.8CrO_x/Al_2O_3 catalysts.

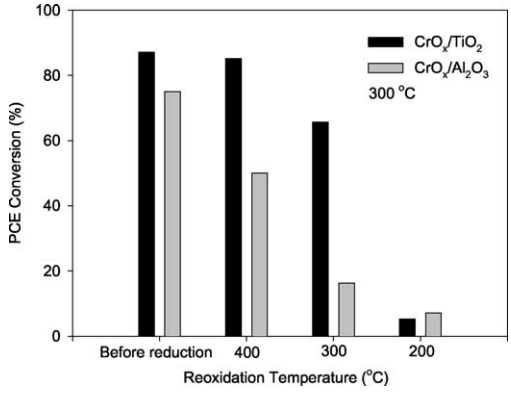

Fig. 9. PCE oxidation activity of 11.9CrO_x/TiO_2 and 10.8CrO_x/Al_2O_3 catalysts with respect to reoxidation temperature.

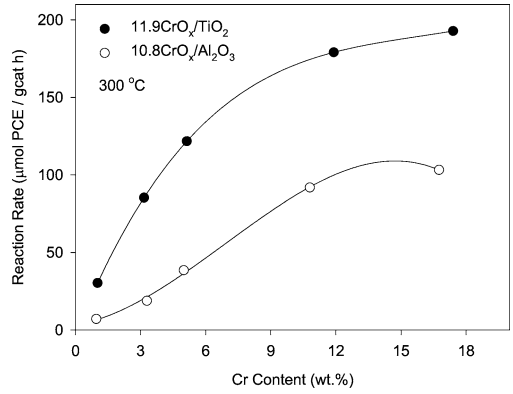

Fig. 10. Reaction rate of PCE oxidation over 11.9CrO_x/TiO_2 and 10.8CrO_x/Al_2O_3 catalysts with respect to Cr content.

as a function of reoxidation temperature can be observed in Fig. 9. The conversion of the catalysts increases as the reoxidation temperature increases. The CrO_x/TiO_2 catalyst reveals relatively higher PCE conversion than CrO_x/Al_2O_3 at the identical reoxidation temperature, particularly at 300 and 400 °C of reoxidation temperatures. This is quite consistent with the amount of hydrogen consumed by TPR as observed in Fig. 8. The result also indicates that the amount of high oxidation state of Cr(VI) on the catalyst surface can be directly correlated with the PCE removal activity. The lower activity of the catalysts reoxidized at 200 °C than that at 300 and 400 °C may be indicative of the effectiveness of Cr(VI) in the present catalytic system.

The reaction rate of the decomposition of PCE over the catalysts containing 1–17.4 wt% of Cr at 300 °C can be examined in Fig. 10. The reaction rate has been calculated on the basis of the differential reactor operation maintaining the PCE conversion less than 15% by controlling the reactor space velocity in order to avoid complexity in the development of the reaction kinetics. The activity by the support itself was minimal compared to the supported catalyst under the reaction conditions covered in the present study. The total reaction rate of the chromium oxide catalyst at steady state is significantly enhanced by the addition of Cr on the surface of the support. It should be noted that CrO_x/TiO_2 always contains a higher reaction rate than CrO_x/Al_2O_3, regardless of the content of Cr on the catalyst surface.

Fig. 11 shows the specific TOF for PCE oxidation over CrO_x/Al_2O_3 at 300 °C with respect to Cr loading. The TOF value was calculated based on the dispersion of Cr on the catalyst surface evaluated by XPS. The result reveals that TOF increases up to 10.8 wt% of Cr content and the further increase of Cr loading decreases the TOF. It should be noted that TOF for CrO_x/TiO_2 catalyst was not obtained due to the applicability of the monolayer model by XPS and the lack of metal dispersion for the catalyst as already stated.

4. Discussion

4.1. Structure of chromium oxide on the catalyst surface

It has been generally recognized that the surface chromium oxide species strongly depends on the support and the surface density of chromium oxide [1]. Based upon observations by XRD, XPS, TPR, and Raman, the features of chromium oxide species on the surface of Al_2O_3 and TiO_2 can be examined with respect to the Cr content.

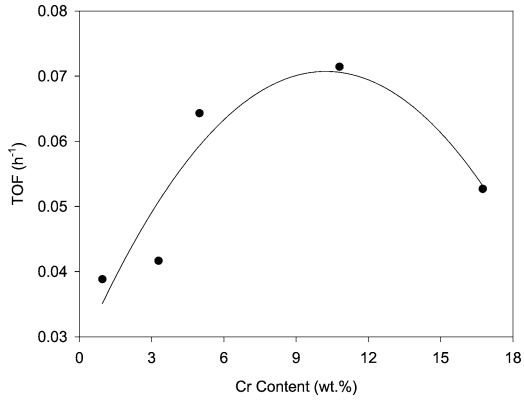

Fig. 11. TOF for PCE oxidation referring to Cr measured by XPS over CrO_x/Al_2O_3 catalysts with respect to Cr content at 300 °C.

The XRD and XPS results for CrO_x/Al_2O_3 and $/TiO_2$ catalysts reveal the general features of chromium oxides on the surface of TiO_2 and Al_2O_3 supports with respect to Cr content. The chromium oxides are well dispersed on the support surface and mainly exist in the form of a high oxidation state of Cr(VI) due to the strong interaction with the support, particularly TiO_2 and Al_2O_3 at a low content of Cr as previously reported [20,23,24]. Adding Cr to the catalyst surface increases the content of Cr(III) on the surface of the catalyst by forming a poorly dispersed cluster of chromium oxide or of crystalline Cr(III) and in part of highly dispersed Cr(III) on the catalyst surface [21]. The distribution of Cr(VI) and Cr(III) on the surface of CrO_x/Al_2O_3 and $/TiO_2$ catalysts is quite consistent with the previous study by Kozlwoski [22] that 60% of Cr existing on the catalyst surface is Cr(VI) at a surface concentration of 3.9 Cr/nm^2 for CrO_x/Al_2O_3. The present result also exhibits the presence of small amount of Cr(III) on the catalyst surface at the lowest loading of Cr, 1 wt% CrO_x/Al_2O_3 (0.4 nm^2) and $/TiO_2$ (0.5 nm^2). This is probably due to the incorporation of the chromium ions onto the lattice of the structure of Al_2O_3 [23] and TiO_2 [7].

The increase of XPS intensity ratios of Cr 2p/Al 2p for a CrO_x/Al_2O_3 catalytic system also confirms that the Cr content on the surface of Al_2O_3 increases in proportion to the amount of Cr added on the catalyst surface. This also implies the uniform deposition of Cr on the Al_2O_3 surface. However, the significant deviation of the intensity ratios between the theoretical values assuming the monolayer coverage and the measured ratios for CrO_x/Al_2O_3 with respect to Cr content as shown in Fig. 3 reveals the dispersion for CrO_x/Al_2O_3 decreasing with increasing Cr loading as listed in Table 2. It can also be concluded from the TPR results revealing an increase of peak intensity of H_2 consumption as the H_2/Cr mole ratio decreases with respect to the content of Cr on the catalyst surface as listed in Table 3.

On the other hand, the trend of XPS intensity ratios of Cr 2p/Ti 2p over the CrO_x/TiO_2 catalyst implies that the monolayer model may not be useful for the impregnated CrO_x/TiO_2 as also observed by Venezia et al. [16]. They discussed that the higher values of the ratio experimentally measured than the theoretical ones with monolayer assumption for CrO_x/TiO_2 contrary to CrO_x/Al_2O_3 are probably due to the location of most of the chromium concentrated on the outside of the titania particles without the diffusion of Cr into the inside of the titania lattice.

Although the identical pretreatment procedure has been employed for stabilizing the chromium species on the surface of TiO_2 and Al_2O_3 with increasing Cr content, the amount of Cr(VI) formed on the surface of CrO_x/Al_2O_3 was higher than that on CrO_x/TiO_2. The quantitative analysis by TPR summarized in Table 3 shows higher hydrogen consumption for CrO_x/Al_2O_3 compared to CrO_x/TiO_2. The XRD patterns also exhibit the presence of crystalline α-Cr_2O_3 only on the surface of $17.4CrO_x/TiO_2$ catalyst. Both results may commonly indicate that the amount of Cr(VI) species stabilized on the surface of Al_2O_3 is higher than that on TiO_2. This also implies that the chromium oxide more easily interacts with the surface of Al_2O_3 than with TiO_2 as Hardcastle and Wachs roughly proposed [3].

The Raman spectra for CrO_x/Al_2O_3 and $/TiO_2$ catalysts may present information on the molecular structure of Cr(VI) existing on the surface of Al_2O_3 and TiO_2. For 1 wt% CrO_x/Al_2O_3 catalyst, only isolated tetrahedral chromate species prevail, which are strongly influenced by the interaction with the surface of the support. When the Cr content increases to 3 wt%, the dimeric chromium oxide species are formed on the surface of the support and further increase of Cr content up to 5 wt% causes the coexistence of dichromate and polychromate including trimers and tetramers. For 10.8 and 16.8 wt% of CrO_x/Al_2O_3, chromium oxide mainly exists in the form of polychromate and the crystalline α-Cr_2O_3 appears at 16.8 wt% of chromium oxide on Al_2O_3, although it has not been observed by XRD. The identification of α-Cr_2O_3 for $16.8CrO_x/Al_2O_3$ catalyst by Raman spectroscopy may reveal that the Raman technique is quite sensitive compared to XRD. The transformation of the molecular structures of Cr including monochromate, dichromate, and polychromate by the increase of the metal content on the catalyst surface was also reported by Vuurman et al. for CrO_x/Al_2O_3 [8].

The CrO_x/TiO_2 catalyst reveals the formation of the polymeric chromium species even at a Cr content as low as 1 wt%, although the coexistence of monomeric species cannot be excluded due to the superimposition of a strong TiO_2 band. It should be noted that Kim and Wachs [9] observed the existence of polymeric chromium oxide species on 1 wt% of chromium oxide catalysts supported on TiO_2, Al_2O_3, ZrO_2, and Nb_2O_5. CrO_x/TiO_x prepared in the present study, however, only shows the formation of polychromate from 1 wt% of Cr content. This may be due to the distinctions of the surface area and the preparation method of the catalysts.

The variety of the molecular structure of chromate species existing on the surface of Al_2O_3 and TiO_2 can also be confirmed by TPR. For the CrO_x/Al_2O_3 catalyst, the shift of TPR peak toward lower temperatures with increasing Cr

content may indicate the strong polymerization of chromium oxide species on Al_2O_3 surface with respect to Cr loading as can be also observed in Raman spectra [35]. The identical peak position of TPR for CrO_x/Al_2O_3 containing 10.8 and 16.8 wt% of Cr may reveal that the degree of polymerization of both catalysts has been saturated on the catalyst surface without further aggregation of metals as consistent with the Raman results as discussed.

Two distinctive reduction peaks for CrO_x/TiO_2 present the existence of two types of chromate species on the catalyst surface. According to Zaki et al. [26], the LTP is related to the more easily reducible polychromate species and the HTP to the less reducible monochromate species. A similar result was also reported by Parlitz et al. [27] assigning the two species as aggregated and isolated Cr(VI) species, respectively. Although additional studies [28,29], especially for CrO_x/SiO_2, reported a two-step reduction from Cr(VI) to Cr(II) via Cr(III), it is not the case for the present study based upon the relative peak intensity of LTP and HTP and the XPS results. It may reflect the formation of polychromate on the surface of CrO_x/TiO_2 containing 1 wt% of Cr content by TPR. It is also quite consistent with the Raman results, although the Raman spectra were obtained under ambient conditions. Therefore, the highly reducible polymeric chromate species are preferentially formed on the surface of TiO_2 compared to Al_2O_3, which is mainly attributed to the stronger interaction of chromium oxide with Al_2O_3 than with TiO_2.

4.2. Redox property of supported chromium oxide catalysts

The redox property of chromia catalyst supported on Al_2O_3 and TiO_2 was observed by sequential study through a TPR1-TPO-TPR2 experiment, hydrogen pulse injection test, and reoxidation of pre-reduced catalyst at 450 °C under H_2 atmosphere to correlate with the PCE oxidation activity. A series of experiments including TPR1-TPO-TPR2 for CrO_x/Al_2O_3 and /TiO_2 show that 70–80% of Cr(VI) existing on the catalyst surface participates in the reversible redox cycle, mainly due to the formation of chromium oxide species such as α-Cr_2O_3 particles that are poorly reversible for the cycle during the course of experiment [30].

The hydrogen pulse test of chromium oxide catalyst as shown in Fig. 7 is useful for confirming the higher reduction rate of CrO_x/TiO_2 catalyst compared to CrO_x/Al_2O_3 as already observed by TPR. The test also reveals that the reduction rate strongly depends on the temperature and the reduction procedure. The reoxidation process accompanying the activation of the oxygen from an oxygen molecule to a reactive O^{2-} species as shown in Fig. 9 also clearly indicates that it occurs more readily over CrO_x/TiO_2 than over CrO_x/Al_2O_3. A similar result was also reported by Sloczynski et al. [31], suggesting the high reoxidation ability of CrO_x/TiO_2 compared to CrO_x/Al_2O_3 mainly due to lower activation energy of the oxidation and stronger capability of electron transfer over CrO_x/TiO_2 than over CrO_x/Al_2O_3.

Based upon the present results, it can be concluded that CrO_x/TiO_2 may contain stronger reduction and oxidation ability than CrO_x/Al_2O_3, which is probably due to the highly polymerized chromium oxide species on the surface of TiO_2 compared to Al_2O_3 by the distinctive metal support interaction.

4.3. Correlation of PCE oxidation activity with structure of chromium oxide

It has been suggested that the high oxidation state of Cr(VI) is an active reaction site for the complete oxidation of PCE based upon the direct relationship between the amount of Cr(VI) existing on the catalyst surface and PCE oxidation activity. This can also be confirmed by the results of Fig. 9, indicating the large amount of Cr(VI) regenerated at the high reoxidation temperature. The higher the content of Cr(VI) on the catalyst surface, the higher the PCE removal activity of the catalyst. Cr(III) species on the catalyst surface relatively reveal weaker catalytic activity than Cr(VI) as clearly observed by the activity of the catalyst reoxidized at 200 °C. However, the quantification of Cr(VI) on the catalyst surface may not be sufficient to elucidate the distinction of the catalytic activity of CrO_x/TiO_2 and /Al_2O_3 catalysts as observed.

The variation of TOF for CrO_x/Al_2O_3 with respect to the content of Cr strongly implies that the active reaction species is closely related to the degree of polymerization of chromium oxide on the catalyst surface. TOF increases as the degree of polymerization of Cr(VI) increases to 10.8 wt% and it levels off to 16.8 wt% of the content of Cr, since the polymerization of Cr(VI) is terminated at 10.8 wt% of Cr where poorly dispersed α-Cr_2O_3 begins to form as examined by Raman and TPR. This may simply indicate that the polymerized chromate is more active than isolated monochromate for the present catalytic system. Since the CrO_x/TiO_2 catalyst more easily forms polychromate with a strong redox capability on its surface than CrO_x/Al_2O_3, the high performance of CrO_x/TiO_2 for the decomposition of PCE over CrO_x/Al_2O_3 can be elucidated. It also suggests that the higher PCE oxidation activity of CrO_x/TiO_2 even containing a smaller amount of Cr(VI) than CrO_x/Al_2O_3 can be closely related to the degree of polymerization of Cr(VI) on the catalyst surface.

The dependence of molecular structure and catalyst support on PCE oxidation activity in the present catalytic system may be elucidated by the role of metal–oxygen–support interaction [12]. Deo and Wocks [13] suggest that the reduction of metal oxide occurs preferentially on the M–O–S (support) bond on the surface of the catalyst. The high reduction temperature of the catalyst is mainly due to the strong bond strength for M–O–S. Based upon MOSI, they studied the oxidation activity of methanol over vanadia-supported catalysts by the determination of the bond strength for V–O–S and observed the reactivity of the catalyst on a variety of the supports in the order of $V_2O_5/ZrO_2 > V_2O_5/TiO_2 >$

$V_2O_5/Nb_2O_5 > V_2O_5/Al_2O_3 > V_2O_5/SiO_2$. Krishnamoorthy et al. [14] recently reported that the catalytic oxidation of 1,2-dichlorobenzene over the transition metal oxides including Cr_2O_3, V_2O_5, MoO_3, Fe_2O_3, and Co_3O_4 supported on TiO_2 and Al_2O_3 is also strongly influenced by MOSI. It has also been observed that the catalytic activity of M_xO_y/TiO_2 is higher than that of M_xO_y/Al_2O_3. This may be also true for the removal of PCE on CrO_x/TiO_2 and $/Al_2O_3$ in the present study.

5. Conclusions

The nature of support and the content of Cr are critical for the molecular structure of chromate species on the surface of the catalyst and the decomposition of PCE. The active reaction species, Cr(VI), increases as the loading of Cr to the catalyst surface increases in the range of Cr content from 1 to 17.4 wt%, while the ratio of Cr(VI)/Cr(III) existing on the surface of the catalyst decreases due to the formation of poorly dispersed α-Cr_2O_3 as the Cr content increases for both chromium oxide catalysts. Raman and TPR revealed that the degree of polymerization of chromate species largely depends on the support employed. The polymerized chromate species were more easily formed on the surface of TiO_2 than on Al_2O_3. The chromium oxide catalyst supported on TiO_2 begins to contain the polymeric chromate species even at a Cr content of 1 wt%, while those on Al_2O_3 are progressively formed on the catalyst surface with respect to the content of Cr. Monochromate is formed at 1 wt% of the Cr content, dichromate at 3.3 wt%, polychromate at 5, 10.8, and 16.8 wt%, and crystalline α-Cr_2O_3 at 16.8 wt%.

The reduction and oxidation ability of chromium oxide catalysts have been significantly enhanced by the polymerization of chromate species on the surface of the catalyst. Highly polymerized chromate species on a TiO_2 surface revealed stronger redox ability compared to monochromate or polymeric chromate species on Al_2O_3.

The overall reaction rate of PCE decomposition increases as the Cr loading increases for both chromium oxide catalysts, although CrO_x/TiO_2 contains a much higher reaction rate compared to CrO_x/Al_2O_3. The TOF of CrO_x/Al_2O_3 catalysts for the present catalytic reaction system increases as the degree of polymerization of chromate increases. It can be concluded that the high PCE oxidation activity of CrO_x/TiO_2 catalyst is mainly due to the presence of more easily reducible polychromate species on surface of TiO_2 compared to CrO_x/Al_2O_3, probably through a metal–oxygen–support interaction.

References

[1] B.M. Weckhuysen, I.E. Wachs, R.A. Schoonheydt, Chem. Rev. 96 (1996) 3327.
[2] M. Cherian, M.S. Rao, A.M. Hirt, I.E. Wachs, G. Deo, J. Catal. 211 (2002) 482.
[3] F.D. Hardcastle, I.E. Wachs, J. Mol. Catal. 46 (1988) 173.
[4] G. Michel, R. Cahay, J. Raman Spectrosc. 17 (1986) 4.
[5] G. Michel, R. Machiroux, J. Raman Spectrosc. 14 (1983) 22.
[6] B. Grzybowska, J. Sloczynski, R. Grabowski, K. Wcislo, A. Kozlowska, J. Stoch, J. Zielinski, J. Catal. 178 (1998) 687.
[7] U. Scharf, H. Schneider, A. Baiker, A. Wokaun, J. Catal. 145 (1994) 464.
[8] M.A. Vuurman, D.J. Stufkens, A. Oskam, J.A. Moulijn, F. Kapteijn, J. Mol. Catal. 60 (1990) 83.
[9] D.S. Kim, I.E. Wachs, J. Catal. 142 (1993) 166.
[10] D.H. Cho, S.D. Yim, G.H. Cha, J.S. Lee, Y.G. Kim, J.S. Chung, I.-S. Nam, J. Phys. Chem. A 102 (1998) 7913.
[11] M.A. Vuurman, I.E. Wachs, D.J. Stufkens, A. Oskam, J. Mol. Catal. 80 (1993) 209.
[12] I.E. Wachs, G. Deo, M.A. Vuurman, H. Hu, D.S. Kim, J.-M. Jehng, J. Mol. Catal. 82 (1993) 443.
[13] G. Deo, I.E. Wachs, J. Catal. 146 (1994) 323.
[14] S. Krishnamoorthy, J.A. Rivas, M.D. Amiridis, J. Catal. 193 (2000) 264.
[15] I.E. Wachs, Catal. Today 27 (1996) 437.
[16] A.M. Venezia, L. Palmisano, M. Schiavello, C. Martin, I. Martin, V. Rives, J. Catal. 147 (1994) 115.
[17] A. Cimino, B.A. De Angelis, A. Luchetti, G. Minelli, J. Catal. 45 (1976) 316.
[18] K. Jagannathan, A. Srinivasan, C.N. Rao, J. Catal. 69 (1981) 418.
[19] C. Wu, F. Wu, L. Chen, X. Huang, Solid State Ionics 152–153 (2002) 335.
[20] Ch. Fountzoula, H.K. Matralis, Ch. Papadopoulou, G.A. Voyiatzis, Ch. Kordulis, J. Catal. 172 (1997) 391.
[21] A. Kytokivi, J.-P. Jacobs, A. Hakuli, J. Merilainen, H.H. Brongersma, J. Catal. 162 (1996) 190.
[22] R. Kozlowski, Bull. Polish Acad. Sci. Chem. 35 (1986) 365.
[23] B.M. Weckhuysen, L.M. De Ridder, P.J. Grobet, R.A. Schoonheydt, J. Phys. Chem. 99 (1995) 320.
[24] F. Cavani, M. Koutyrev, F. Trifiro, A. Bartolini, D. Ghisletti, R. Iezzi, A. Santucci, G. Del Piero, J. Catal. 158 (1996) 236.
[25] D. Cordischi, M. Cristina Campa, Indovina, M. Occhiuzz, J. Chem. Soc., Faraday Trans. 90 (1994) 207.
[26] M.I. Zaki, N.E. Fouad, G.C. Bond, S.F. Tahir, Thermochim. Acta 285 (1996) 167.
[27] B. Parlitz, W. Hanke, R. Fricke, M. Richter, U. Roost, G. Hlmann, J. Catal. 94 (1985) 24.
[28] L.I. Ilieva, D.H. Andreeva, Thermochim. Acta 265 (1995) 223.
[29] A. Hakuli, M.E. Harlin, L.B. Backman, A.O. Krause, J. Catal. 184 (1999) 349.
[30] B.M. Weckhuysen, L.M. De Ridder, R.A. Schoonheydt, J. Phys. Chem. 97 (1993) 4756.
[31] J. Sloczynski, B. Grzybowska, R. Grabowski, A. Kozlowska, K. Wcislo, Phys. Chem. Chem. Phys. 1 (1999) 333.
[32] L.A. Grunes, Phys. Rev. B 27 (1983) 2111.
[33] F.W. Lytle, R.B. Greegor, G.L. Bibbins, K.Y. Blohowiak, R.E. Smith, G.D. Tuss, Corros. Sci. 37 (1995) 349.
[34] F.E. Huggins, M. Najih, G.P. Huffman, Fuel 78 (1999) 233.
[35] B.M. Weckhuysen, R.A. Schoonhetdt, J.-M. Jehng, I.E. Wachs, S.J. Cho, R. Ryoo, S. Kijlstra, E. Poels, J. Chem. Soc., Faraday Trans. 91 (1995) 3245.
[36] S.D. Yim, K.-H. Chang, D.J. Koh, I.-S. Nam, Y.G. Kim, Catal. Today 63 (2000) 215.
[37] J.J. Spivey, Ind. Eng. Chem. Res. 26 (1987) 2165.
[38] S.D. Yim, K.-H. Chang, I.-S. Nam, Hwahak Konghak (J. Korean Inst. Chem. Eng.) 39 (2001) 265.
[39] S.D. Yim, D.J. Koh, I.-S. Nam, Y.G. Kim, Catal. Lett. 64 (2000) 201.
[40] F.P.J.M. Kerkhof, J.A. Moulijn, J. Phys. Chem. 83 (1979) 1612.
[41] P.W. Park, J.S. Ledford, Langmuir 13 (1997) 2726.
[42] J.H. Scofield, J. Electron Spectrosc. Relat. Phenom. 8 (1976) 129.
[43] D.R. Penn, J. Electron Spectrosc. Relat. Phenom. 9 (1976) 29.